J Neuropathol Exp Neurol
Vol. 75, No. 5, May 2016, pp. 415–428
doi: 10.1093/jnen/nlw017

ORIGINAL ARTICLE

Complement and Humoral Adaptive Immunity in the Human Choroid Plexus: Roles for Stromal Concretions, Basement Membranes, and Epithelium

G. R. Wayne Moore, MD, FRCPC, FRCPath, Cornelia Laule, PhD, Esther Leung, MSc, Vladimira Pavlova, BMLSc, B. Paul Morgan, MB, PhD, FRCPath, and Margaret M. Esiri, DM, FRCPath

Abstract

The choroid plexus (CP) provides a barrier to entry of toxic molecules from the blood into the brain and transports vital molecules into the cerebrospinal fluid. While a great deal is known about CP physiology, relatively little is known about its immunology. Here, we show immunohistochemical data that help define the role of the CP in innate and adaptive humoral immunity. The results show that complement, in the form of C1q, C3d, C9, or C9neo, is preferentially deposited in stromal concretions. In contrast, immunoglobulin (Ig) G (IgG) and IgA are more often found in CP epithelial cells, and IgM is found in either locale. C4d, IgD, and IgE are rarely, if ever, seen in the CP. In multiple sclerosis CP, basement membrane C9 or stromal IgA patterns were common but were not specific for the disease. These findings indicate that the CP may orchestrate the clearance of complement, particularly by deposition in its concretions, IgA and IgG preferentially via its epithelium, and IgM by either mechanism.

From the Department of Pathology and Laboratory Medicine (GRWM, CL, EL, VP); Department of Radiology, University of British Columbia (CL); Vancouver General Hospital, Vancouver Coastal Health Authority (GRWM); International Collaboration on Repair Discoveries (ICORD), Blusson Spinal Cord Centre (GRWM, CL, EL, VP), Vancouver, BC, Canada; Institute of Infection and Immunity, Cardiff University, Henry Wellcome Building, Heath Park, Cardiff, UK (BPM); and Neuropathology Department, University of Oxford, John Radcliffe Hospital, Oxford, UK (MME).

Send correspondence to: G. R. Wayne Moore, MD, FRCPC, FRCPath, International Collaboration on Repair Discoveries (ICORD), Room 5200, Blusson Spinal Cord Centre, 818 West 10th Avenue, Vancouver, BC V5Z 1M9, Canada; E-mail: wayne.moore@vch.ca

This study was supported by the Multiple Sclerosis Society of Canada (GRWM and CL).

Dr Moore is a member of the Medical Advisory Committee of the Multiple Sclerosis Society of Canada. His research is supported by grants from the Multiple Sclerosis Society of Canada. He has received a grant-in-aid of research from Berlex Canada, acted as a consultant for Schering, and received an honorarium from Teva. Dr Morgan is a Consultant for GSK. Margaret M. Esiri was in receipt of financial support from the UK NIHR via the Oxford Biomedical Research Centre during the preparation of this manuscript.

Supplementary Data can be found at http://www.jnen.oxfordjournals.org.

Key Words: Cerebrospinal fluid, Choroid plexus, Complement; Concretions, Immunoglobulins, Immunology, Multiple sclerosis.

INTRODUCTION

The choroid plexus (CP) is a frond-like structure projecting into the cerebrospinal fluid (CSF) of the ventricular system of the brain. It is comprised of a simple cuboidal epithelium resting on a basement membrane (BM) overlying a fibrovascular stroma (Figs. 1, 2A–C) (1). Patrolling the ventricular surface of the CP epithelium are epiplexus cells (Kolmer cells), which are thought to be macrophages (2). Stromal blood vessels possess fenestrated endothelia (1). The CP stroma and BM are therefore exposed to circulating molecules (Fig. 2D), the barrier to their entry to the CSF being at the level of CP epithelial cells. The morphologic basis for this blood–CSF barrier is in the form of tight junctions between adjacent epithelial cells (Fig. 1), in a manner similar to the blood–brain barrier at the level of the CNS endothelium (3, 4). The fibrous component of the stroma shows varying degrees of collagen compaction, some focal regions being intensely sclerotic and, in many instances, calcified (Fig. 2C). Up to now, these sclerotic structures (which we refer to as "concretions") have not been emphasized. These structures are hyalinized and somewhat irregular in shape and differ from psammoma bodies, which are well-delineated spherical, somewhat laminated, often larger structures that tend to be clustered and presumably originate within the remnants of the leptomeningeal embryologic contribution to the CP.

The best-known role of the CP is the production of CSF (5) (Fig. 1), which provides buoyancy for the brain in the rigid skull and for the spinal cord in the vertebral column. The CSF also serves as a strategically placed intermediary for the passage of molecules into and out of the CNS (Fig. 1). Thus, utilizing a myriad of molecular transporters, it transports specific molecules from the blood into the CSF, many of these having trophic effects on the CNS both during development and in adult life (6–8) (Fig. 1). The CP also has a system of efflux transporters that remove waste products and toxic substances from the CSF (9) (Fig. 1).

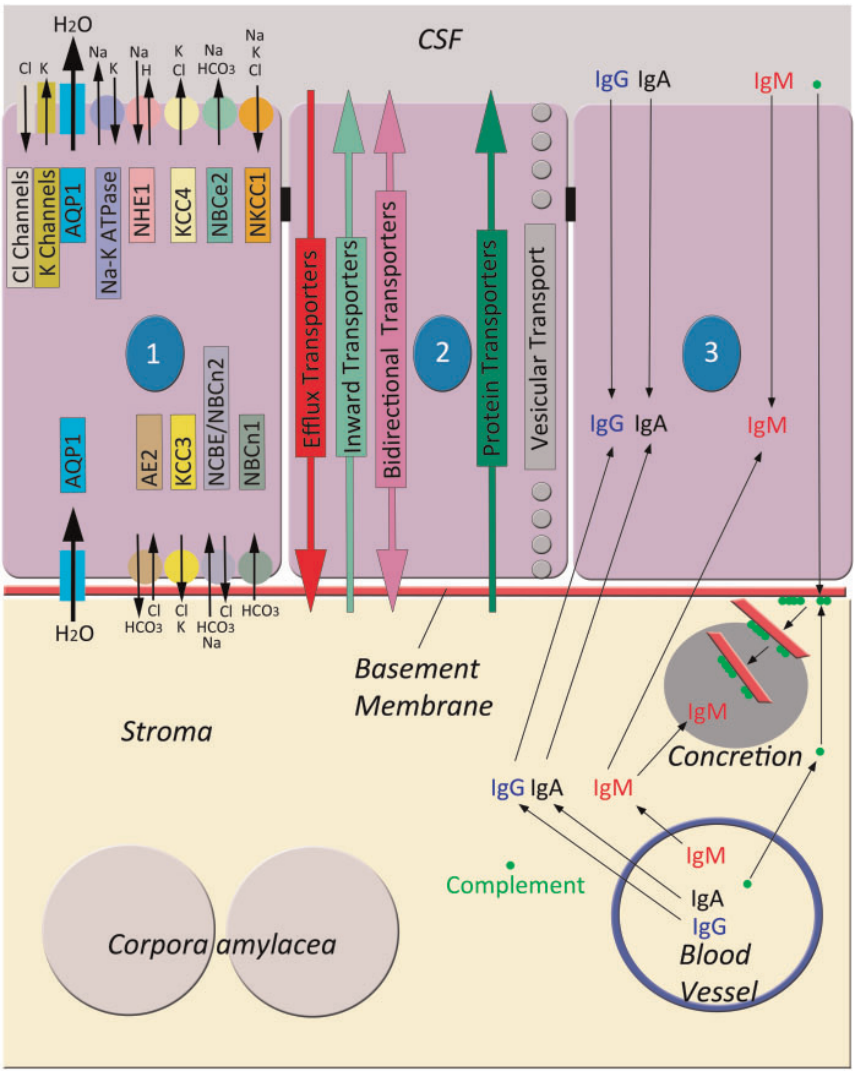

FIGURE 1. Schematic diagram of directionality of ions and molecules in the choroid plexus (CP). Three CP epithelial cells (cytoplasm in purple, nuclei in blue, numbered by nucleus), joined by tight junctions (small black rectangles), rest on a basement membrane (red) overlying the stroma. In the stroma, there are corpora amylacea, a blood vessel, and a concretion. Cell 1 illustrates ionic channels (rectangles with directional arrows) and pumps (small circles with directional arrows), color coded to match their respective names. They are positioned in the apical or basolateral cell membrane as indicated. Their combined effect is responsible for cerebrospinal fluid (CSF) production, creating an osmotic gradient that causes a net movement of water from the extracellular space of the stroma, through the epithelial cell cytoplasm, and into the ventricle via AQP1 water channels. Carbonic anhydrase (not shown) is the major enzyme responsible for the generation of H^+ and HCO_3^-. For a review of ionic channels and pumps and their role in CSF formation, see Damkier et al (5). Cell 2 shows the transport systems for larger molecules. These comprise the efflux transporters that transport substances (particularly lipid compounds) out of the CSF, inward transporters that transport relatively small molecules into the CSF, bidirectional transporters that transport molecules in either direction, and protein transporters that transport individual specific proteins into the CSF. Some substances are transported in vesicles. For a review of transporters in the CP, see Saunders et al (7). Cell 3, its associated basement membrane, underlying stroma, and stromal blood vessel show postulated mechanisms of handling complement and immunoglobulin (Ig). The thin black arrows indicating directionality of movement are speculative. Our results would suggest that complement (green dots) from serum or CSF is frequently deposited in concretions by associating with the basement membrane that is eventually incorporated into the concretion. Our data also indicate that IgM is also deposited in concretions but may also be handled by epithelial cells, whereas IgA and IgG are predominately handled by epithelial cells. Abbreviations: AE2, anion exchanger 2 (Cl^-/HCO_3^- exchanger); AQP1, aquaporin-1 water channel; Cl, chloride ions (Cl^-); H, hydrogen ions (H^+); HCO_3, bicarbonate ion (HCO_3^-); K, potassium ions (K^+); KCC3 and KCC4, K^+–Cl^- cotransporter 3 and 4; Na, sodium ions (Na^+); Na-K ATPase, Na^+-K^+ ATPase; NBC, Na^+–HCO_3^- cotransporters; NCBE, Na^+-dependent Cl^-/HCO_3^- exchanger; NHE1, Na^+/H^+ exchanger 1; NKCC1, Na^+-K^+-$2Cl^-$ cotransporter 1. Adapted from Figure 11 in Damkier HH, Brown PD, Praetorius J. Cerebrospinal fluid secretion by the choroid plexus. Physiol Rev 2013:93;1847–92 and Figure 2 in Saunders NR, Daneman R, Dziegielewska KM, Liddelow SA. Transporters of the blood-brain and blood-CSF interfaces in development and in the adult. Mol Aspects Med 2013:34;742–52.

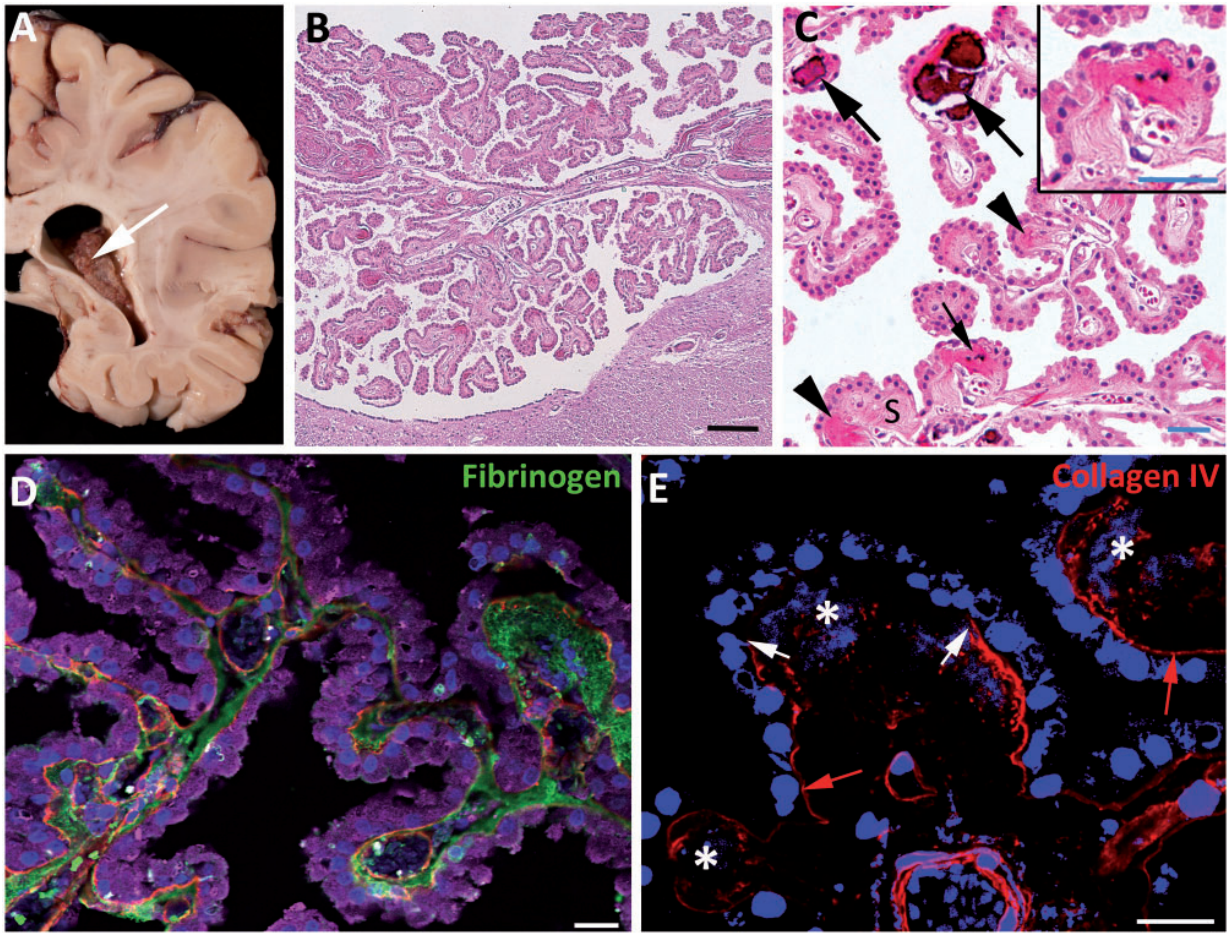

FIGURE 2. Macroscopic and microscopic features of the choroid plexus (CP). **(A)** The CP is a frond-like structure (white arrow), shown here in the lateral ventricle. **(B)** Micrograph of hematoxylin and eosin (H&E) stain shows the CP is a papillary structure comprised of a cuboidal epithelium and a fibrovascular stroma. **(C)** Under higher magnification, the cuboidal structure of the epithelial cells, as well as the fibrous tissue and vasculature of the stroma (S), is evident. In the stroma, there are several concretions comprised of dense fibrous tissue (black arrowheads), some of which show calcification, varying from early (small black arrow, and shown at higher magnification in inset) to advanced (large black arrows). **(D)** The normal permeability of CP blood vessels is evident by the extravasation of high molecular weight molecules, in this case fibrinogen (green), into the stroma. The basement membrane is stained for collagen IV (red); epithelial cells are stained for transthyretin (purple). Cell nuclei are stained with 4′,6-diamidino-2-phenylindole (DAPI) (blue). **(E)** Confocal immunofluorescence demonstrates 3 concretions (asterisks) as irregularly blue-staining regions when the DAPI (blue) brightness is enhanced. The concretions show the incorporation of basement membrane material (red, stained for collagen IV), which normally is located just beneath the epithelium (red arrows). The middle concretion is associated with a defect (between the white arrows) in the subepithelial basement membrane, which also shows thickening adjacent to the right edge of the defect. The concretion on the right shows thickening and duplication of the overlying subepithelial basement membrane. The basement membrane is also normally seen in the walls of stromal blood vessels (in cross-section in the lower middle and in longitudinal section in the lower right of the panel). Scale bars: white = 20 μm; blue = 50 μm; black = 200 μm.

Over recent years, it has become increasingly evident that the CP has a pivotal role in the cellular immunology of the CNS (10). In contrast to many of the tenets of the long-standing notion of immunological privilege of the CNS, it is now widely accepted that T lymphocytes regularly track through the CNS as part of their immune-surveillance mandate (11). These are predominately central memory T cells (12), which are confined to the CSF and do not enter the parenchyma. Once the immune response is activated after antigen presentation to T cells within the subarachnoid space, the recruitment of effector T cells to the endothelium, and thence the perivascular space and their entry into the CNS parenchyma through the previously impenetrable glia limitans, can occur (13). T cells may enter the CP stroma via P-selectin and intercellular adhesion molecule-1, which are expressed on stromal venular endothelia (14). The entry portal from the stroma through the CNS barriers for the initial wave of Th17 cells (currently regarded as an important T-cell subset in the

mediation of autoimmune demyelination) is the CP epithelium; this may apply to other T-cell subtypes, including T regulatory cells (15, 16). The migration is thought to be mediated by the interaction of the cytokine receptor CCR6 on T cells with its ligand CCL20 on CP epithelial cells. Other receptor ligand interactions, such as those involving epithelial V-like antigen (17), have also been proposed as mechanisms for entry of T cells across the CP epithelium. It has also been suggested that, in addition to the entrance of inflammatory cells and the well-known negative effects of inflammation in the CNS, some T cells and macrophages with trophic or positive effects on the CNS may also enter via the CP (18, 19). However, a shift of T cells in the CP epithelium to a Th2 phenotype in senescence is associated with cognitive decline mediated by the chemokine CCL11 (20). In addition to these local phenomena, it has also been shown that CP genes respond to acute (21) and chronic (22) inflammatory events occurring outside the CNS, and this may be the explanation for the effect of systemic inflammation on the manifestations of neurodegenerative disorders (21, 22). Furthermore, the CP is responsive to T regulatory cells, and this may also be important in the regulation of clearance of amyloid-β by inflammatory cells in experimental Alzheimer disease (23). Thus, there is ample evidence that the CP has a key role in CNS T-cell trafficking, with resultant negative and positive influences on the CNS.

While most of the findings described above are from studies in experimental animals, there have been only a few that examined cellular immunity in the human CP. A study of the CP in multiple sclerosis (MS) showed upregulation of Class II MHC on macrophages in the stroma and epithelium, similar to encephalitis, and CD68-negative cells in the stroma thought to be dendritic cells (24). Scattered T cells, in relation to CP vessels (somewhat fewer than in cases of encephalitis), were evident in MS, whereas none were noted in noninflammatory controls. The findings were consistent with the entry of inflammatory cells though the CP in MS patients and were present even in the chronic progressive stages of the disease (24).

Complement, which is part of the innate immune system, provides one of the first defenses against microorganisms and mediates the elimination of apoptotic or degenerating cells (25); it also interacts with the adaptive immune response (26), where, among other functions, it participates in the recruitment and activation of lymphocytes and neutrophils (26, 27). Complement comprises a cascade of interacting components that generates proinflammatory triggers culminating in formation of the cytolytic membrane attack complex (MAC).

In the human CP, complement localization has been described in schistosomiasis (28), cirrhosis (29), Alzheimer disease (30), hypertension (31), and on apoptotic CP epithelial cells in diabetic ketoacidosis (32). Complement receptor (CR) 1 mRNA has been detected in CP epithelial cells (33), and CR3 induction in epiplexus cells has been detected after experimental high-altitude exposure (34). Complement regulators membrane cofactor protein (CD46) (33, 35), decay accelerating factor (CD55), and CD59 (33) have also been documented in CP epithelia. There is upregulation of these complement regulators by CP epithelial cells in bacterial meningitis (36).

In experimental animals, complement deposition has been detected in the CP in mesangiocapillary glomerulonephritis in lambs (37), spontaneous immune complex disease in rats (38), experimental autoimmune encephalomyelitis (EAE) in guinea pigs (39, 40), serum sickness in mice and rats (41, 42), and experimental trypanosomiasis in mice (43).

Interestingly, the gene for the receptor for C5a is constitutively expressed on neurons in the mouse brain (44). Moreover, in the presence of systemically circulating lipopolysaccharide endotoxin, the genes for the receptor for C3a, as well as C3 and C5, are upregulated in regions without a blood–brain barrier, such as the CP (44). These findings in the mouse would indicate that there is a system in the CP that is primed for complement production in the event of systemic insults such as endotoxemia. This then raises the issue of the elimination of complement and the targets to which it may be complexed from the CNS and how complement may be controlled or inactivated to prevent bystander parenchymal damage beyond that required to eliminate the offending target.

In addition to the participation of individual complement components in the complement cascade that culminates in the MAC, certain components, particularly C5a, have a chemotactic effect on neutrophils and, as such, contribute to the formation of cellular inflammatory infiltrates.

In contrast to complement, the adaptive immune system, a component of which is the humoral immune response of immunoglobulins synthesized by B cells and their derivatives, is antigen specific. Immunoglobulins have also been detected in the human CP in various conditions. These include neurologically normal individuals (45), autoimmune nephritis in Goodpasture syndrome (46), IgA nephropathy (47), systemic lupus erythematosus (48–51), subacute bacterial endocarditis (52), acquired immunodeficiency syndrome (53), cirrhosis (29), Alzheimer disease (30), and hypertension (31). Immunoglobulin light chains have been detected in the psammoma bodies and the stroma of the CP (54); the stromal depositions in the last report appear to correspond to the concretions described in the current study.

In experimental animals, CP immunoglobulin has been demonstrated in normal hamsters (55), spontaneous lupus-like syndrome in nude mice (56), mesangiocapillary glomerulonephritis in lambs (37), spontaneous immune complex disease (38), subcutaneous inoculation of an antigen (horseradish peroxidase) (57, 58), systemic injection of antibodies to proteins (58, 59), acute and chronic serum sickness (42, 60, 61), EAE (39, 40), experimental malaria (62), and experimental trypanosomiasis (43).

From the above, it is clear that immunoglobulins and complement may be evident in the CP in many circumstances, including conditions that are not usually considered to have an immune or autoimmune pathogenesis. It would seem, therefore, that their appearance in the CP is not specific, and most likely the CP acts as a depository for immune complexes and complement. Until now, an extensive systematic study of the occurrence of immunoglobulins and complement in the human CP in a range of disorders to determine if there is any difference in the anatomic distribution of these two arms of the immune response has not been carried out to our knowledge. In this study, we found that immunoglobulin and complement

deposition in the CP is exceedingly common. In fact, in one form or another, this was found in the CP in virtually every case, regardless of the associated clinical circumstances.

Thus, while a great deal is known about CP physiology, until recently, relatively little attention has been paid to its immunology. These studies have revealed important insights into the involvement of the CP in immunity (63). Moreover, the predisposition of MS plaques to be proximal to CSF pathways raises the possibility that CP barrier or filter dysfunction have important roles in this disorder (64). For these reasons, we examined the immunohistochemical localization of representative components of the complement cascade and of all immunoglobulins in the CP in MS patients and in a variety of neurological and nonneurological control conditions. The data show a consistent deposition of complement in the stromal concretions regardless of the clinical setting. On the other hand, immunoglobulins tended to localize to epithelial cells. These findings suggest segregation of the respective mechanisms of handling products of the innate and humoral arms of the immune system within the CP.

MATERIALS AND METHODS

Tissue Samples

Formalin-fixed paraffin-embedded CP samples from institutionally approved, next of kin–consented autopsies on 13 MS patients (Table 1, cases 1–13), 24 other neurological conditions (Table 1, cases 14–37), and 11 nonneurological conditions (Table 1, cases 38–48) were initially immunohistochemically stained using primary antibodies to immunoglobulin (Ig) G, IgA, IgM, IgD, IgE, C1q, C3d, C4d, C9, and a neoepitope on C9 (C9neo) specific for the terminal MAC (Table 2). To determine whether a trend noted in this series for IgA and C9 was consistent for MS patient samples, an additional 11 cases of MS (Table 1, cases 49–59), 19 cases of other neurological conditions (Table 1, cases 60–78), and 5 cases of nonneurological conditions (Table 1, cases 79–83) were also studied for IgA, C9, and C9neo.

Immunofluorescence

Three-micrometer-thick formalin-fixed paraffin sections on 1:10 polylysine (Sigma-Aldrich, St Louis, MO)-coated slides were deparaffinized in xylene, dehydrated in absolute ethanol, and washed with distilled water. Depending on the primary antibody, sections were either treated with proteinase K for 6–9 minutes or microwaved in citrate buffer (pH 6.0) for 2 minutes at 90% power, 2 minutes at 70% power, 6 minutes at 50% power, and cooled to room temperature over 20 minutes (Table 2). To reduce autofluorescence, they were treated with 1% (weight/volume) sodium borohydride (Fisher Scientific, Fair Lawn, NJ). They were then incubated with 5% normal donkey serum, the same species as the secondary antibody, for 30 minutes. The primary antibody (Table 2) was applied overnight at room temperature, followed by washing in phosphate-buffered saline with 0.5% Tween (PBS-Tween). All primary antibodies are known to recognize the appropriate antigen in formalin-fixed paraffin-embedded tissue. Negative controls consisted of immunoglobulins of the same subtype in the same dilution from the same, but unimmunized, species as the primary antibody (Table 2). Fluorescent secondary antibodies (Invitrogen [Life Technologies]/Molecular Probes, Burlington, ON, Canada) were applied at a dilution of 1:400 for 180 minutes in the dark (Table 2) and then washed in PBS-Tween. DAPI (4′,6-diamidino-2-phenylindole, Invitrogen) at 1:400 dilution was applied for 10 minutes as a nuclear counterstain, followed by coverslipping with ProLong Gold antifade mounting medium (Invitrogen). Slides were examined with a Leica DM4000 B fluorescence microscope (Leica Microsystems, Wetzlar, Germany).

Staining Analysis

The anatomical localizations of staining for each primary antibody were recorded as follows: epithelial cells (EP), subepithelial basement membrane (BM), stippled staining of BM (BMs), BM overlying concretion (BMc), concretion (C), stroma (S), and stromal vasculature (V). Statistical comparisons between MS, other neurological conditions, and nonneurological conditions were carried out for each primary antibody based on the presence of staining at locations in the CP using a 2-tailed Fisher exact test with Bonferroni correction for 70 multiple comparisons ($p < 0.0007$, SPSS Statistics 17.0). Statistical comparisons between the presence of each primary antibody in relation to every other antibody in both the concretions and the epithelial cells were carried out using a 2-tailed Fisher exact test with Bonferroni correction for 45 multiple comparisons ($p < 0.001$). Finally, the percent positivity of each antibody in the concretions versus the epithelial cells was compared with a 2-tailed Fisher exact test with Bonferroni correction for 10 multiple comparisons ($p < 0.005$).

Confocal Microscopy

Selected sections were stained with a multiple-labeling procedure. This comprised one of the above primary antibodies combined with an antibody to collagen IV (to highlight basement membranes) and an antibody to transthyretin (to highlight CP epithelium) in a cocktail, followed by a cocktail of the appropriate secondary antibodies. The same section preparation procedures, washes, concentrations, and timeframe as described above for the individual antibodies were employed. DAPI was again used as the nuclear counterstain. Sections were imaged in a Zeiss Axio-observer Z1 spinning-disc confocal microscope (Carl Zeiss Microscopy, Oberkochen, Germany). Deconvolution was carried out using a nearest-neighbor algorithm. Images were brightened x 50 in Photoshop CS5.1 (Adobe Systems Inc., San Jose, CA).

RESULTS

Autofluorescence of Formalin-Fixed Paraffin-Embedded Tissues

Strong autofluorescence of red blood cells was invariably present in all sections (test sections and negative controls). Supplemental Digital Content shows examples of autofluorescence and test slides referenced to negative controls. In addition, Biondi bodies (or ring bodies) (65), small thread-like

TABLE 1. Summary of Cases for Series 1 and Series 2

Series 1: C1q, C3d, C4d, C9, C9neo, IgA, IgG, IgM, IgD, IgE					Series 2: IgA, C9, C9neo				
Case[a]	Age	Sex	PMI	Diagnosis	Case[a]	Age	Sex	PMI	Diagnosis
1	32y	F	1d	MS	49	76y	M	?R	MS
2	40y	M	NK	MS	50	74y	F	2d	MS, AD
3	57y	F	NK	MS	51	54y	F	4d	MS
4	49y	F	NK	MS	52	51y	F	12h	MS
5	35y	M	17h	MS	53	76y	F	12h	MS
6	79y	M	NK	MS	54	78y	M	?R	MS (acute on chronic)
7	58y	M	3d	MS	55	55y	M	3d	MS
8	71y	F	NK	MS	56	45y	F	?R	MS, arachnoid cysts
9	57y	F	NK	MS	57	41y	F	?R	MS
10	76y	M	NK	MS	58	67y	F	NK	MS
11	56y	F	NK	MS	59	33y	M	NK	MS
12	33y	F	NK	MS	60	41y	M	2h	Neuroaxonal leukodystrophy
13	51y	F	1d	MS	61	64y	F	1d	B-cell lymphoma
14	19y	F	NK	Acute disseminated encephalomyelitis	62	61y	M	2d	CADASIL
15	24y	F	1d	Subacute sclerosing panencephalitis	63	57y	M	2d	Mild hydrocephalus, mild Purkinje cell loss, steatosis
16	74y	F	3d	Arteriolo, CAA	64	80y	M	5d	DLBD, tau pvent glia, pallidotomy, bilat STN stimulation
17	77y	F	1d	Remote spinal cord injury	65	84y	F	3d	AD, arteriolo, état criblé
18	81y	M	3d	Arteriolo, lacunes, poss AD	66	68y	F	2d	Cerebral atrophy NYD, MI, renal cysts
19	83y	F	3d	Motor neuron disease	67	33y	F	2d	Metastatic ca, mild anoxic encep, lymphocytic thyroiditis
20	71y	M	1d	Remote berry aneurysm clipping	68	50y	F	1d	Sarcoma, chemo, DIC, gram-neg sepsis, anoxic encep
21	70y	M	4d	AD	69	35y	F	2d	Liver transplant, systemic Herpes simplex (not CNS), CPM
22	17y	F	21h	Hepatic cerebral edema	70	21y	M	2d	Hemochromatosis, hepatic failure, ? pvent demyelin, SCO
23	79y	M	2.5d	Mastocytosis with encephalopathy	71	70y	M	1d	Poss AD, CAA, hydro, arteriolo, anoxic encep, MI, steatosis
24	61y	F	NK	Intravascular lymphoma	72	83y	F	1d	Old frontal infarct, abdominal aortic aneurysm, steatosis
25	61y	M	1.5d	IgA nephropathy, IC-hypotension, cirrhosis	73	75y	M	4d	Prob AD, CAA, mild pvent WM pallor, liver fibrosis, CAD
26	64y	M	3d	AD	74	56y	F	2d	Cereb infarcts, leiomyosarcoma, hypereosinophilia
27	53y	F	1d	TIAs, pseudomembranous colitis	75	58y	F	1d	EtOH cerebellar degen, sepsis, DIC, pancreatitis, steatosis
28	74y	M	4h	Basilar aneurysm clipping, hepatic abscesses	76	77y	F	2d	Meningioma NS, subacute and old cereb infarcts, PSP
29	81y	M	3d	Old cereb infarcts, CAD	77	63y	F	2d	Anoxic encep, panhypopituitarism, hypertension
30	89y	M	2d	Old vertebrobasilar infarcts	78	72y	M	4d	Poss AD, pvent WM pallor, meningeal fibrosis, Ca lung
31	76y	F	1d	Old cereb infarcts, CAD, pseudomemb colitis	79	69y	M	4d	Hepatic failure, sclerosing peritonitis
32	54y	M	5h	Anoxic encephalopathy, pancreatitis	80	44y	F	1d	Diffuse B-cell lymphoma (not CNS), steatosis
33	71y	F	NK	AD, CAA	81	54y	F	2d	Polycystic kidney and liver, portal vein thrombosis
34	62y	F	2d	CML, prob vasculitis, spinal cord infarct	82	48y	F	1d	Myocarditis
35	62y	F	1d	Cerebral B-cell lymphoma	83	80y	M	2d	Cardiac surgery, Hepatic steatosis and fibrosis
36	54y	M	1d	Prev medulloblast NS, old cereb infarcts					
37	51y	F	3d	NHL, cyclosporin, rxed PRES					
38	60y	F	7h	Metastatic breast Ca					
39	59y	M	3d	Prob Wegener's granulomatosis					
40	56y	M	3d	Tacrolimus treatment, Liver transplant					
41	62y	M	3d	HPL, T-cell Lymphoma					
42	57y	M	4d	Aortic Aneurysm					
43	32y	F	1d	Pancreatitis, IBS, Asthma					
44	74y	M	18h	Hepatic Abscess, Crohn's Disease					
45	41y	F	3d	Endocarditis, Cirrhosis					
46	71y	M	3d	MI, Arteriolo					
47	49y	F	4d	Ovarian and Breast Ca					
48	59y	M	2d	Hepatocellular Ca					

AD, Alzheimer disease; Arteriolo, arteriolosclerosis; bilat, bilateral; Ca, carcinoma; CAA, cerebral amyloid angiopathy; CAD, atherosclerotic coronary artery disease; CADASIL, cerebral autosomal dominant arteriopathy with subacute infarcts and leukoencephalopathy; Cbll, cerebellar; Cereb, cerebral; chemo, chemotherapy; CML, chronic myelogenous leukemia; CNS, central nervous system; CPM, central pontine myelinolysis; d, day(s); degen, degeneration; demyelin, demyelination; DIC, disseminated intravascular coagulation; DLBD, diffuse Lewy body disease; encep, encephalopathy; EtOH, alcoholic; F, female; h, hours; HPL, hemophagocytic lymphohistiocytosis; hydro, hydrocephalus; IBS, irritable bowel syndrome; IC, intracranial; M, male; medulloblast, medulloblastoma; MI, myocardial infarct; MS, multiple sclerosis; neg, negative; NHL, non-Hodgkin's lymphoma; NK, not known; NS, neurosurgery; NYD, not yet diagnosed; PMI, postmortem interval; poss, possible; PRES, posterior reversible encephalopathy syndrome; Prev, previous; Prob, probable; pseudomemb, pseudomembranous; PSP, progressive supranuclear palsy; pvent, periventricular; rx'ed, treated; SCO, Sertoli-cell-only syndrome; STN, subthalamic nucleus; TIAs, transient ischemic attacks; WM, white matter; ?R, PMI not available, referred-in-case; y, years.

[a]MS: cases 1–13,49–59; other neurological conditions: cases 14–37,60–78; nonneurological conditions: cases: 38–48,79–83.

TABLE 2. Primary Antibodies and Normal Sera

Primary Antibodies	Source (and Product Code; Location)	Antigen Retrieval	Secondary Antibody
IgA: rabbit polyclonal IgG (1:4000)	Dako (A0262); Glostrup, Denmark	Microwave	Alexa Fluor 488 donkey anti-rabbit IgG (H+L)
IgG: goat polyclonal IgG (1:10,000)	Biogenesis Technology (5172-2104); Poole, UK	Microwave	Alexa Fluor 488 donkey anti-goat IgG (H+L)
IgM: mouse monoclonal IgG1κ (1:500)	Dako (M0702)	Microwave	Alexa Fluor 488 donkey anti-mouse IgG (H+L)
IgD: mouse monoclonal IgG1κ (1:500)	Dako (M0703)	Microwave	Alexa Fluor 488 donkey anti-mouse IgG (H+L)
IgE: mouse monoclonal IgG (1:400)	Affinity Bio Reagents (SA1-19260); Golden, CO	Microwave	Alexa Fluor 488 donkey anti-mouse IgG (H+L)
C1q: rabbit polyclonal (1:20)	BioGenex (AR100-5R); San Ramon, CA	Microwave	Alexa Fluor 488 donkey anti-rabbit IgG (H+L)
C3d: rabbit polyclonal (1:2000)	Dako (A0063)	Microwave	Alexa Fluor 488 donkey anti-rabbit IgG (H+L)
C4d: mouse monoclonal IgGκ (1:250)	Quidel Corporation (A213); San Diego, CA	Microwave	Alexa Fluor 488 donkey anti-mouse IgG (H+L)
C9: sheep polyclonal IgG (1:800)	Abcam Inc (ab53896); Cambridge, MA	Microwave	Alexa Fluor 488 donkey anti-sheep IgG (H+L)
C9neo: mouse monoclonal IgG1 (1:100)	B. P. Morgan (Clone B7); Cardiff, UK	Proteinase K	Alexa Fluor 488 donkey anti-mouse IgG (H+L)
Collagen IV: mouse IgG1 (1:100)	Abcam Inc (ab49213)	Microwave	Alexa Fluor 568 donkey anti-mouse IgG (H+L)
Collagen IV: rabbit IgG (1:500)	Abcam Inc (ab6586)	Microwave	Alexa Fluor 568 donkey anti-rabbit IgG (H+L)
Transthyretin: sheep IgG (1:2000)	Abcam Inc (ab9015)	Microwave	Alexa Fluor 647 donkey anti-sheep IgG (H+L)
Transthyretin: chicken polyclonal IgY (1:400)	Abcam Inc (ab106558)	Microwave	Alexa Fluor 647 donkey anti-chicken IgG (H+L)
Normal Sera			
Normal rabbit serum IgG fraction	Dako (X0903)	Microwave	Alexa Fluor488 donkey anti-rabbit IgG(H+L)/ Alexa Fluor568 donkey anti-rabbit IgG (H+L)
Normal mouse serum IgG $_1\kappa$	Sigma-Aldrich (M9269); St Louis, MO	Microwave/ proteinase K	Alexa Fluor 488 donkey anti-mouse IgG (H+L)
Normal goat serum purified IgG	Sigma-Aldrich (I5256)	Microwave	Alexa Fluor 488 donkey anti-goat IgG (H+L)
Normal sheep serum	Sigma-Aldrich (S3772)	Microwave	Alexa Fluor 488 donkey anti-sheep IgG(H+L)/ Alexa Fluor 647 Donkey anti-Sheep IgG (H+L)
Normal chicken serum	Jackson Immuno Research Labs (003-000-120); West Grove, PA	Microwave	Alexa Fluor 647 donkey anti-chicken IgG (H+L)
Normal donkey serum 5% w/v	Sigma-Aldrich (D9663)		

linear, curvilinear, or spherical inclusions in CP epithelial cells, which express amyloid and accumulate with aging, also autofluoresce (Supplementary Data). Thus, these sources of brilliant autofluorescence were ignored when examining the test sections.

Concretions and the Subepithelial BM

Strands of collagen IV–positive material in addition to its immediate subepithelial location were frequently found deep within the concretion (Fig. 2E), particularly near its epithelial pole. In proximity to the concretion, the BM staining was often attenuated, discontinuous, thickened, or duplicated (Figs. 2E, 3B, F–H).

Complement Deposition

For C1q, the first component in the classical complement pathway, we frequently noted positivity in the CP stroma, in concretions (Fig. 3A), and associated with the BM, particularly overlying concretions (Table 3). Epithelial cells were sometimes positive (Fig. 3A; Table 3). This was associated with nearby C1q-positive ependymal cells (Fig. 3A and inset). Stromal blood vessels were occasionally positive.

C3d was deposited in concretions and often in a diffuse or multifocal fashion in the stroma and associated with BM overlying concretions (Fig. 3B; Table 3). Vascular C3d staining was unusual (Table 3).

Immunofluorescence for C4d, a product of activation of both the classical and lectin complement pathways, was usually negative, aside from occasional BM-associated deposits. The concretions were rarely positive (Table 3).

C9 showed relatively consistent staining of concretions (Fig. 3C, F; Table 3). C9 positivity was infrequently observed in the stroma, but stromal vascular staining was relatively frequent. In contrast to C3d, in which the BM deposits generally tended to be uniform and located particularly over concretions, C9 frequently showed BM positivity in an irregular stippled pattern not necessarily associated with concretions (Fig. 3C–E; Table 3).

Staining for C9neo, which is specific for the MAC, was frequently detected in concretions where staining was evident either in their center or periphery (Fig. 3G, H; Table 3). BM staining was evident (Table 3), but was generally not as obvi-

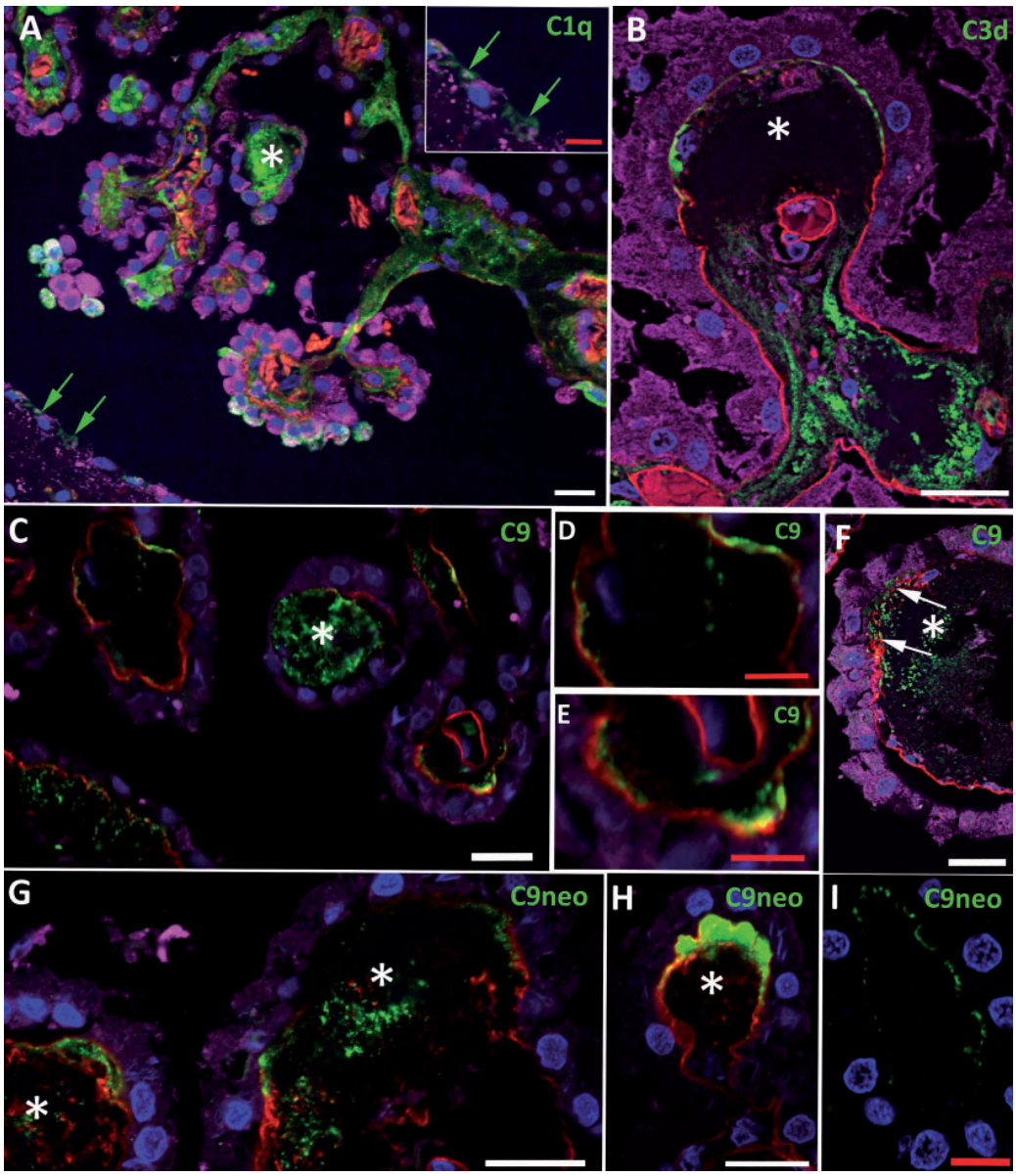

FIGURE 3. Complement deposition in the choroid plexus (CP). Complement components (green) are shown in relation to the CP epithelium (transthyretin in purple), basement membrane (collagen IV in red), cell nuclei (DAPI in blue), and stromal concretions (asterisks). **(A)** C1q is seen in the CP stroma, a concretion, the cytoplasm of some epithelial cells, and some nearby ependymal cells (green arrows, shown at higher magnification in inset). **(B)** C3d is present in the stroma and in the superficial aspects of a concretion; the overlying subepithelial basement membrane is discontinuous and focally incorporated into the concretion. **(C)** C9 is evident in a concretion and is deposited adjacent to the basement membrane, with which it directly colocalizes (embeds within) only rarely (yellow). **(D)** High magnification of the upper left of panel **C,** showing C9 deposited adjacent to, but not directly colocalizing with (embedded within), subepithelial basement membrane; stippled pattern of C9 deposition shown on the left. **(E)** High magnification of the lower right of panel **C**, showing stippled C9 deposition adjacent to subepithelial basement membrane but only focally directly colocalizing with (embedded within) it (yellow). **(F)** C9 is present in a concretion and is deposited adjacent to the overlying subepithelial basement membrane, which is both focally interrupted (between the white arrows) and thickened in this region. **(G)** Two concretions show deposition of C9neo, with interruption (right concretion) and thickening (right and left concretions) of the overlying subepithelial basement membrane, which is also incorporated into their deeper structures. **(H)** A prominent C9neo deposition in the superficial aspect of a concretion and adjacent to a discontinuous subepithelial basement membrane, with which there is focal direct colocalization (yellow). **(I)** Staining for only C9neo (counterstained for nuclei) shows delicate subepithelial basement membrane-associated deposits. Scale bars: white = 20 μm; red = 10 μm.

TABLE 3. Percentage of Cases Positive for Complement

C′	Percent Positive; p Value	EP	BM	BMs	BMc	C	S	V	Any
C1q	Percent positive MS	8	46	0	62	77	100	38	100
	Percent positive non-MS	66	51	6	69	89	80	31	97
	p value	0.007	> 0.999	> 0.999	0.74	0.37	0.17	0.74	> 0.999
C3d	Percent positive MS	0	54	0	69	100	92	38	100
	Percent positive non-MS	3	49	6	91	100	94	3	100
	p value	> 0.999	> 0.999	> 0.999	0.08	> 0.999	> 0.999	0.004	> 0.999
C4d	Percent positive MS	0	15	0	23	8	0	0	31
	Percent positive non-MS	6	31	0	14	14	0	0	40
	p value	> 0.999	> 0.999	> 0.999	0.66	> 0.999	> 0.999	> 0.999	0.74
C9	Percent positive MS	21	4	71	38	96	13	67	100
	Percent positive non-MS	7	3	42	31	98	10	83	98
	p value	0.112	> 0.999	0.03	0.61	0.50	0.71	0.14	> 0.999
C9 neo	Percent positive MS	13	17	4	4	67	8	21	75
	Percent positive non-MS	7	16	0	3	79	14	21	81
	p value	0.41	> 0.999	0.29	> 0.999	0.26	0.72	> 0.999	0.56

Any, staining of any of the following components of the choroid plexus; BM, epithelial basement membrane staining; BMc, staining of epithelial basement membrane overlying concretion; BMs, stippled staining of epithelial basement membrane; C, staining of concretion; EP, epithelial cell staining; S, staining of stroma; V, staining of stromal vasculature.
$p < 0.0007$ after Bonferroni correction.

ous as staining with the antibody to the C9 component and the earlier components of the cascade; by confocal microscopy, this manifested as minute discrete punctate deposits adjacent to or in the BM (Fig. 3I). Vasculature staining was occasionally seen but epithelial and stromal staining was less frequent.

Complement components were detected in concretions with a significantly higher frequency than in epithelial cells ($p < 0.0001$, Fig. 5). Overall, the complement components that were frequently deposited in the CP were more likely found in concretions than immunoglobulins; this was significant (Fig. 5). The close association of complement components with BM was confirmed by their spatial relationship to collagen IV (Fig. 3B–F, H, I), but direct colocalization indicating complement embedment in BM was infrequent (Fig. 3E, H).

Localization of Immunoglobulins

Generally, staining for immunoglobulin isotypes showed a great deal of variability, ranging from negative to focal positivity. Because they circulate in the serum, they also, not unexpectedly, showed focal positivity in the stroma (Fig. 4A–C; Table 4); BM associated with (Fig. 4A) and unassociated with (Fig. 4B, C) concretions (Table 4). CP rarely showed staining for IgD or IgE (Table 4).

In contrast to complement, IgA and IgG were only occasionally positive in concretions but were more frequently evident in epithelial cells ($p < 0.0001$) (Fig. 4A, B; Table 4). IgM had no particular preference for either of these locales (Fig. 4C, D; Table 4). When each of the tested molecules was compared to one another, epithelial cell staining was seen for IgA and IgG more often than for IgM, C3d, C9, and C9neo; these differences were significant (Fig. 5). Epithelial cells more superficially in the CP and closer to C1q-positive or immunoglobulin-positive ependymal cells often tended to be positive for C1q or immunoglobulins, whereas deeper cells were negative (Figs. 3A, 4B).

No Pattern of Complement or Immunoglobulin Is Specific for MS

We were initially struck by a diffuse stromal and BM IgA or a diffuse stippled BM C9 deposition in cases of MS. Therefore, we expanded the study to include more cases stained for IgA, C9, and C9neo and found these patterns still tended to be seen more often in MS than in other conditions, but this was not a statistically significant difference (Tables 3, 4). A reverse trend was noted for C1q in epithelial cells. These patterns were seen in MS cases irrespective of the presence of actively demyelinating or silent plaques.

DISCUSSION

Complement Preferentially Localizes in CP Concretions

Our results show the consistent deposition of complement components (except C4d, which was only rarely evident in the CP) in the stromal concretions of the CP. Complement components that were frequently deposited in the CP were significantly more commonly found in concretions than in epithelial cells ($p < 0.005$). This suggests that the concretion is an important depot for complement deposition and offers an important function for these previously unexplored structures. Complement frequently had a spatial relationship to collagen IV (Fig. 3C, E), but its direct colocalization with this BM marker was infrequent (Fig. 3C), indicating that complement may be adherent to the BM without necessarily impregnating it. The existence of collagen IV–positive material within concretions suggests that BM material was incorporated within them. Moreover, BM absence, duplication, or thickenings at the epithelial pole of the concretion are also consistent with active BM involvement in the function of this structure. The findings are somewhat analogous to the deposition of complement in the glomerular subepithelial space or outer aspect of

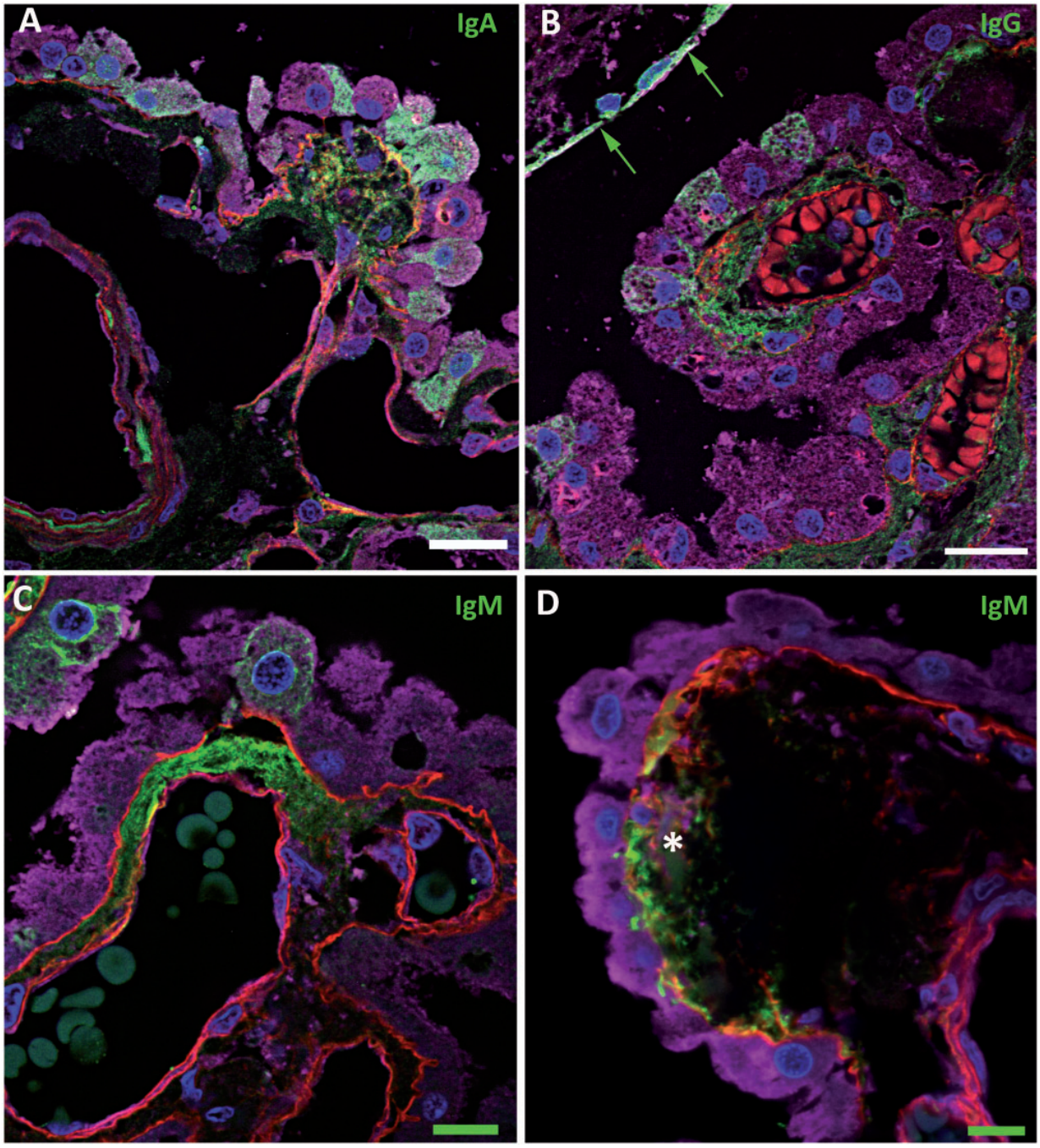

FIGURE 4. Immunoglobulins in the choroid plexus. Confocal micrographs showing immunoglobulins in green, basement membrane (collagen IV) in red, epithelial cells (transthyretin) in purple, and cell nuclei (DAPI) in blue. **(A)** IgA (green) is seen in the stroma, focally colocalizing in the subepithelial basement membrane (yellow), and in the cytoplasm of epithelial cells. **(B)** IgG (green) is evident in the stroma and in some epithelial cells near IgG-positive ependymal cells (green arrows). **(C)** IgM (green) is focally evident in the stroma and in some epithelial cells. **(D)** IgM deposition in a concretion (asterisk), which is associated with a defect in the overlying subepithelial basement membrane. There is focal basement membrane thickening within which there is colocalization with IgM (yellow). Some basement membrane material is also seen within the concretion. Scale bars: green = 10 μm; white = 20 μm.

A

Marker	% positive for concretions	% positive for EP	p-value
IgA	24	66	< 0.0001
IgG	25	69	< 0.0001
IgM	35	21	0.173
IgD	0	2	> 0.999
IgE	0	6	0.242
C1q	85	50	0.0004
C3d	100	2	< 0.0001
C4d	13	4	0.268
C9	98	11	< 0.0001
C9neo	76	9	< 0.0001

B Summary of p-values for Concretions

	IgA	IgG	IgM	IgD	IgE	C1q	C3d	C4d	C9	C9neo
IgA										
IgG	> 0.999									
IgM	0.227	0.374								
IgD	0.0001	0.0002	< 0.0001							
IgE	0.0001	0.0002	< 0.0001	> 0.999						
C1q	< 0.0001	< 0.0001	< 0.0001	< 0.0001	< 0.0001					
C3d	< 0.0001	< 0.0001	< 0.0001	< 0.0001	< 0.0001	0.012				
C4d	0.119	0.19	0.016	0.026	0.026	< 0.0001	< 0.0001			
C9	< 0.0001	< 0.0001	< 0.0001	< 0.0001	< 0.0001	0.012	0.532	< 0.0001		
C9neo	< 0.0001	< 0.0001	< 0.0001	< 0.0001	< 0.0001	0.263	0.0001	< 0.0001	< 0.0001	

C Summary of p-values for Epithelial Cells

	IgA	IgG	IgM	IgD	IgE	C1q	C3d	C4d	C9	C9neo
IgA										
IgG	0.8									
IgM	< 0.0001	< 0.0001								
IgD	< 0.0001	< 0.0001	0.008							
IgE	< 0.0001	< 0.0001	0.07	0.4						
C1q	0.095	0.096	0.005	< 0.0001	< 0.0001					
C3d	< 0.0001	< 0.0001	0.008	> 0.999	0.362	< 0.0001				
C4d	< 0.0001	< 0.0001	0.027	> 0.999	0.677	< 0.0001	> 0.999			
C9	< 0.0001	< 0.0001	0.13	0.092	0.535	< 0.0001	0.092	0.327		
C9neo	< 0.0001	< 0.0001	0.059	0.257	0.746	< 0.0001	0.257	0.484	0.793	

FIGURE 5. Choroid plexus concretion and epithelial cell (EP) staining. Significant differences are highlighted in green. Any statistically significant comparisons for C4d, IgD, and IgE are attributable to the rarity of staining of these compared with the other complement components and immunoglobulins. **(A)** Concretion staining was observed more often than EP staining for C1q, C3d, C9, and C9neo. The reverse was true for IgA and IgG. There was no significant difference in the frequency between concretion and EP staining for IgM. **(B)** There were significant differences in staining frequencies of concretions (more frequent, see Tables 3 and 4) for C1q, C3d, C9, and C9neo than for IgA, IgG, and IgM. **(C)** There were significant differences in staining frequency of epithelial cells for IgG and IgA (more frequent, see Tables 3 and 4) than for IgM C3d, C9, and C9 neo. Two-tailed Fisher exact test, Bonferroni correction for multiple comparisons (SPSS Statistics 17.0).

the BM in membranous glomerulonephritis and the subsequent reaction of the BM in that disorder (66). There is also a striking similarity to complement localization in the choroid (which could be considered to be the equivalent of CP stroma) and Bruch's membrane (possibly the retinal equivalent of the CP epithelial BM) (67). Furthermore, there is also complement deposition in drusen (68), which may be analogous to the CP concretions described here. In the retina, these findings have been implicated in the pathogenesis of macular degeneration (69). However, in the CP, these phenomena are presumably not pathogenic because they are exceedingly frequent and evident even in nonimmune noninflammatory conditions. It is, however, certainly possible that their progression is associated with aging or age-related degeneration of the CP.

TABLE 4. Percentage of Cases Positive for Immunoglobulins

Ig	Percent Positive; p Value	EP	BM	BMs	BMc	C	S	V	Any
IgA	Percent positive MS	79	79	0	46	42	75	4	96
	Percent positive non-MS	61	54	0	29	17	32	0	88
	p value	0.13	0.05	> 0.999	0.20	0.02	0.001	0.29	0.43
IgG	Percent positive MS	69	62	0	38	31	69	0	77
	Percent positive non-MS	69	46	0	49	23	40	0	77
	p value	> 0.999	0.52	> 0.999	0.75	0.71	0.11	> 0.999	> 0.999
IgM	Percent positive MS	8	85	0	31	15	85	0	92
	Percent positive non-MS	26	46	0	31	43	60	0	80
	p value	0.25	0.022	> 0.999	> 0.999	0.099	0.17	>.999	0.42
IgD	Percent positive MS	0	0	0	0	0	0	0	0
	Percent positive non-MS	3	0	0	0	0	3	0	3
	p value	> 0.999	> 0.999	> 0.999	> 0.999	> 0.999	> 0.999	> 0.999	> 0.999
IgE	Percent positive MS	0	0	0	0	0	0	0	0
	Percent positive non-MS	9	6	0	0	0	0	0	12
	p value	0.55	> 0.999	> 0.999	> 0.999	> 0.999	> 0.999	> 0.999	0.56

Any, staining of any of the following components of the choroid plexus; BM, epithelial basement membrane staining; BMc, staining of epithelial basement membrane overlying concretion; BMs, stippled staining of epithelial basement membrane; C, staining of concretion; EP, epithelial cell staining; S, staining of stroma; V, staining of stromal vasculature.
$p < 0.0007$ after Bonferroni correction.

We hypothesize that complement within the stroma that is derived from either the serum or the CSF is initially attracted to and adherent to the BM, and the latter, with the attached complement, is internalized within the concretion (Fig. 1), which over time undergoes dystrophic calcification. C9neo, indicating the complement cascade had been activated to completion resulting in the terminal MAC, was demonstrated in the BM and concretions. Since C9 neoantigens are expressed both in the MAC and in the soluble terminal complex, C9neo staining is firm evidence of activation of complement to completion and means that cells in the vicinity will have been exposed to the MAC. It is suggested that the deposition of this complex within the BM and subsequently in the concretion would be a means of preventing it from causing damage to CNS cells. It is possible that many of the earlier components of the complement cascade detected in various compartments of the CP, including the concretion, represent individual components or parts of complexes that have failed to activate later components to complete the cascade. Another and even more intriguing explanation is that the aggregation of the components of complement is occurring in situ in the CP, the immunohistochemistry demonstrating their generation at various stages. In this interpretation, the concretions may be regarded as markers of previous complement-mediated destruction in the CP. In either scenario, the data are consistent with complement being trapped in the BM and the concretion.

Immunoglobulins Preferentially Localize in CP Epithelium

In contrast to complement, IgA and IgG were only occasionally positive in concretions but were more frequently evident in epithelial cells ($p < 0.005$). IgM, the immunoglobulin produced earlier than IgA and IgG in the adaptive immune response, appears to have no particular preference for either of these locales. When each of the tested molecules were compared to one another, epithelial cell staining was seen with IgA and IgG significantly more often than IgM, C1q, C3d, C9, and C9neo. Staining frequently was seen only in scattered epithelial cells, rather than in a diffuse fashion throughout the epithelium. Epithelial cells that were more superficially located in the CP and closer to C1q-positive or immunoglobulin-positive ependymal cells often tended to be positive for C1q or immunoglobulins, whereas deeper cells were negative, suggesting that C1q and immunoglobulin were being actively removed from the ventricular CSF. However, directionality cannot be stated with certainty based on this morphological data alone. Nevertheless, substantiating this interpretation is the finding that, in experimental animals, transport of IgG across the CP is largely an efflux system (CSF to blood) rather than in the other direction (3, 70). Because serum molecules may diffuse in small quantities through the blood–brain and blood–CSF barriers (8, 71), the findings suggest that the CP epithelial cells may serve to recycle these leaked proteins to the circulation by transporting them from the CSF into the CP serum-rich stroma. The finding of IgG positivity in CP epithelial cells is not new, having been reported in the human neonate (72, 73). Our results indicate that this is also an adult phenomenon and that this location is highly characteristic of immunoglobulins.

Despite the fenestration of vessels in the CP stroma, the finding of immunoglobulins in the stroma was not consistent. Interestingly, in a study of EAE, IgG was detected in the CP stroma in animals given complete Freund's adjuvant, with or without the immunogen, but not in controls, suggesting that systemic inflammatory signals may be necessary to produce increased permeability above baseline in these vessels to allow extravasation of the immunoglobulin (74). By inference, this may indicate that stromal immunoglobulin may be a reflection of systemic inflammation. In this regard, we initially noted a diffuse stromal and BM IgA or a diffuse stippled BM C9 deposition in MS cases. In light of this finding, we expanded the

study to include more MS and non-MS cases stained for IgA and C9 and found these patterns tended to be seen in MS more than other conditions, but this was not a significant difference. It is possible that both these trends may be explained by systemic inflammation, for example pulmonary or urinary infections, to which patients with advanced MS are particularly susceptible. Nevertheless, the trend raises the possibility that these phenomena in the CP may be relevant to the immunopathogenesis of some cases of MS. This may also be true of the trend toward decreased C1q staining in epithelial cells in MS. These trends might have been clarified if we had clinical information about the MS cases, but unfortunately, these were often unavailable to us.

The CP as a Possible Systemic Immunologic Filter

This study further defines the role of the CP in humoral and innate immunity. Detoxification and complement and immune complex removal have largely been attributed to organs such as the liver and spleen (75, 76). Our results would suggest that the CP, by utilizing trapping mechanisms employed by its epithelial cells, BM, and concretions, may serve a similar role for the brain, protecting it from immune-mediated and other potentially toxic systemic threats. It is also possible that similar functions may be ascribed to other CNS concretion-like structures, such as corpora amylacea (77) and psammoma bodies for the compaction or disposal of degraded endogenous molecules and toxic compounds that have already made their way to the CNS parenchyma or leptomeninges, respectively. We hope that this study, which represents static snapshots in time imaged by immunofluorescence, will spawn immunological, physiological, and molecular approaches to test and refine further the hypotheses generated by our data. Furthermore, the possibility that these CP clearance functions are also systemically important for the entire organism, not just the brain in which it is strategically poised, is also an important consideration worthy of further exploration.

ACKNOWLEDGMENTS

The authors thank Steve Kalloger for statistical advice. We thank the families who donated tissue of their loved ones for this research and the Oxford Brain Bank, which supplied some of this tissue.

REFERENCES

1. Strazielle N, Ghersi-Egea JF. Choroid plexus in the central nervous system: Biology and physiopathology. J Neuropathol Exp Neurol 2000;59:561–74
2. Ling EA, Kaur C, Lu J. Origin, nature, and some functional considerations of intraventricular macrophages, with special reference to the epiplexus cells. Microsc Res Tech 1998;41:43–56
3. Strazielle N, Ghersi-Egea JF. Physiology of blood-brain interfaces in relation to brain disposition of small compounds and macromolecules. Mol Pharm 2013;10:1473–91
4. Engelhardt B, Sorokin L. The blood-brain and the blood-cerebrospinal fluid barriers: Function and dysfunction. Semin Immunopathol 2009;31:497–511
5. Damkier HH, Brown PD, Praetorius J. Cerebrospinal fluid secretion by the choroid plexus. Physiol Rev 2013;93:1847–92
6. Lehtinen MK, Bjornsson CS, Dymecki SM, et al. The choroid plexus and cerebrospinal fluid: Emerging roles in development, disease, and therapy. J Neurosci 2013;33:17553–9
7. Saunders NR, Daneman R, Dziegielewska KM, et al. Transporters of the blood-brain and blood-CSF interfaces in development and in the adult. Mol Aspects Med 2013;34:742–52
8. Smith DE, Johanson CE, Keep RF. Peptide and peptide analog transport systems at the blood-CSF barrier. Adv Drug Deliv Rev 2004;56:1765–91
9. Spector R. Nature and consequences of mammalian brain and CSF efflux transporters: Four decades of progress. J Neurochem 2010;112:13–23
10. Meeker RB, Williams K, Killebrew DA, et al. Cell trafficking through the choroid plexus. Cell Adh Migr 2012;6:390–6
11. Hickey WF. Migration of hematogenous cells through the blood-brain barrier and the initiation of CNS inflammation. Brain Pathol 1991;1:97–105
12. Provencio JJ, Kivisäkk P, Tucky BH, et al. Comparison of ventricular and lumbar cerebrospinal fluid T cells in non-inflammatory neurological disorder (NIND) patients. J Neuroimmunol 2005;163:179–84
13. Engelhardt B, Ransohoff RM. Capture, crawl, cross: The T cell code to breach the blood-brain barriers. Trends Immunol 2012;33:579–89
14. Kivisäkk P, Mahad DJ, Callahan MK, et al. Human cerebrospinal fluid central memory CD4+ T cells: Evidence for trafficking through choroid plexus and meninges via P-selectin. Proc Natl Acad Sci U S A 2003;100:8389–94
15. Reboldi A, Coisne C, Baumjohann D, et al. C-C chemokine receptor 6-regulated entry of T_H17 cells into the CNS through the choroid plexus is required for the initiation of EAE. Nat Immunol 2009;10:514–23
16. Sallusto F, Impellizzieri D, Basso C, et al. T-cell trafficking in the central nervous system. Immunol Rev 2012;248:216–27
17. Wojcik E, Carrithers LM, Carrithers MD. Characterization of epithelial V-like antigen in human choroid plexus epithelial cells: Potential role in CNS immune surveillance. Neurosci Lett 2011;495:115–20
18. Baruch K, Schwartz M. CNS-specific T cells shape brain function via the choroid plexus. Brain Behav Immun 2013;34:11–6
19. Schwartz M, Baruch K. The resolution of neuroinflammation in neurodegeneration: Leukocyte recruitment via the choroid plexus. EMBO J 2014;33:7–22
20. Baruch K, Ron-Harel N, Gal H, et al. CNS-specific immunity at the choroid plexus shifts toward destructive Th2 inflammation in brain aging. Proc Natl Acad Sci U S A 2013;110:2264–9
21. Marques F, Sousa JC, Coppola G, et al. Kinetic profile of the transcriptome changes induced in the choroid plexus by peripheral inflammation. J Cereb Blood Flow Metab 2009;29:921–32
22. Marques F, Sousa JC, Coppola G, et al. The choroid plexus response to a repeated peripheral inflammatory stimulus. BMC Neurosci 2009;10:135
23. Baruch K, Rosenzweig N, Kertser A, et al. Breaking immune tolerance by targeting $Foxp3^+$ regulatory T cells mitigates Alzheimer's disease pathology. Nat Commun 2015;6:7967
24. Vercellino M, Votta B, Condello C, et al. Involvement of the choroid plexus in multiple sclerosis autoimmune inflammation: A neuropathological study. J Neuroimmunol 2008;199:133–41
25. Ricklin D, Hajishengallis G, Yang K, et al. Complement: A key system for immune surveillance and homeostasis. Nat Immunol 2010;11:785–97
26. Morgan BP, Marchbank KJ, Longhi MP, et al. Complement: Central to innate immunity and bridging to adaptive responses. Immunol Lett 2005;97:171–9
27. Price PJ, Banki Z, Scheideler A, et al. Complement component C5 recruits neutrophils in the absence of C3 during respiratory infection with modified vaccinia virus Ankara. J Immunol 2015;194:1164–8
28. Pittella JE, Bambirra EA. Histopathological and immunofluorescence study of the choroid plexus in hepatosplenic schistosomiasis mansoni. Am J Trop Med Hyg 1989;41:548–52
29. Pittella JE, Bambirra EA. Immune complexes in the choroid plexus in liver cirrhosis. Arch Pathol Lab Med 1991;115:220–2
30. Serot JM, Bene MC, Faure GC. Comparative immunohistochemical characteristics of human choroid plexus in vascular and Alzheimer's dementia. Hum Pathol 1994;25:1185–90
31. Pittella JE, Bambirra EA. Immune complexes in the choroid plexus in systemic hypertension. J Clin Pathol 1988;41:1245–6
32. Hoffman WH, Casanova MF, Cudrici CD, et al. Neuroinflammatory response of the choroid plexus epithelium in fatal diabetic ketoacidosis. Exp Mol Pathol 2007;83:65–72

33. Singhrao SK, Neal JW, Rushmere NK, et al. Differential expression of individual complement regulators in the brain and choroid plexus. Lab Invest 1999;79:1247–59
34. Wang D, Kaur C. Response of epiplexus cells associated with the choroid plexus in the lateral ventricles of adult rats to high altitude exposure. Neurosci Lett 2000;285:197–200
35. McQuaid S, Cosby SL. An immunohistochemical study of the distribution of the measles virus receptors, CD46 and SLAM, in normal human tissues and subacute sclerosing panencephalitis. Lab Invest 2002;82: 403–9
36. Canova C, Neal JW, Gasque P. Expression of innate immune complement regulators on brain epithelial cells during human bacterial meningitis. J Neuroinflammation 2006;3:22
37. Gardiner AC. Mesangiocapillary glomerulonephritis in lambs. III. Quantitative and qualitative aspects of immunopathology. J Pathol 1976;119: 11–9
38. Lampert PW, Oldstone MB. Host immunoglobulin G and complement deposits in the choroid plexus during spontaneous immune complex disease. Science 1973;180:408–10
39. Grundke-Iqbal I, Lassmann H, Wisniewski HM. Chronic relapsing experimental allergic encephalomyelitis. Immunohistochemical studies. Arch Neurol 1980;37:651–6
40. Koh CS, Tsukada N, Yanagisawa N, et al. Mild encephalitogenic activity of basic protein–acidic lipid complex from myelin and detection of immune complexes in experimental allergic encephalomyelitis. J Neuroimmunol 1981;1:69–80
41. Lampert P, Garrett R, Lampert A. Ferritin immune complex deposits in the choroid plexus. Acta Neuropathol 1977;38:83–6
42. Peress NS, Miller F, Palu W. The immunopathophysiological effects of chronic serum sickness on rat choroid plexus, ciliary process and renal glomeruli. J Neuropathol Exp Neurol 1977;36:726–33
43. Poltera AA, Hochmann A, Rudin W, et al. Trypanosoma brucei brucei: A model for cerebral trypanosomiasis in mice—An immunological, histological and electronmicroscopic study. Clin Exp Immunol 1980;40: 496–507
44. Nadeau S, Rivest S. The complement system is an integrated part of the natural innate immune response in the brain. FASEB J 2001;15:1410–2
45. Olsson JE, Link H. Distribution of serum proteins and beta-trace protein within the nervous system. J Neurochem 1973;20:837–46
46. McIntosh RM, Copack P, Chernack WB, et al. The human choroid plexus and autoimmune nephritis. Arch Pathol 1975;99:48–50
47. Woodroffe AJ. IgA, glomerulonephritis and liver disease. Aust N Z J Med 1981;11:109–11
48. Boyer RS, Sun NC, Verity A, et al. Immunoperoxidase staining of the choroid plexus in systemic lupus erythematosus. J Rheumatol 1980;7: 645–50
49. Gershwin ME, Hyman LR, Steinberg AD. The choroid plexus in CNS involvement of systemic lupus erythematosus. J Pediatr 1975;87:588–90
50. Sher JH, Pertschuk LP. Immunoglobulin G deposits in the choroid plexus of a child with systemic lupus erythematosus. J Pediatr 1974;85:385–7
51. Brentjens J, Ossi E, Albini B, et al. Disseminated immune deposits in lupus erythematosus. Arthritis Rheum 1977;20:962–8
52. Davis JA, Weisman MH, Dail DH. Vascular disease in infective endocarditis. Report of immune-mediated events in skin and brain. Arch Intern Med 1978;138:480–3
53. Falangola MF, Castro-Filho BG, Petito CK. Immune complex deposition in the choroid plexus of patients with acquired immunodeficiency syndrome. Ann Neurol 1994;36:437–40
54. Jovanovic I, Ugrenovic S, Vasovic L, et al. Immunohistochemical and morphometric analysis of immunoglobulin light-chain immunoreactive amyloid in psammoma bodies of the human choroid plexus. Anat Sci Int 2014;89:71–8
55. Sakiyama H, Yamaguchi K, Chiba K, et al. Biochemical characterization and tissue distribution of hamster complement C1s. J Immunol 1991; 146:183–7
56. Monier JC, Costa O, Souweine G, et al. Lupus-like syndrome in some strains of nude mice. Thymus 1980;1:241–55
57. Fleury J, Bellon B, Bernaudin JF, et al. Electron-microscopic immunohistochemical study of the localization of immunoglobulin G in the choroid plexus of the rat. Cell Tissue Res 1984;238:177–82
58. Baloyannis SJ, Gonatas NK. Distribution of anti-HRP antibodies in the central nervous system of immunized rats after disruption of the blood brain barrier. J Neuropathol Exp Neurol 1979;38:519–31
59. Huang JT, Mannik M, Gleisner J. In situ formation of immune complexes in the choroid plexus of rats by sequential injection of a cationized antigen and unaltered antibodies. J Neuropathol Exp Neurol 1984;43:489–99
60. Brentjens JR, O'Connell DW, Albini B, et al. Experimental chronic serum sickness in rabbits that received daily multiple and high doses of antigen: A systemic disease. Ann N Y Acad Sci 1975;254:603–13
61. McCombe PA, Pender MP. Lack of neurological abnormalities in Lewis rats with experimental chronic serum sickness. Clin Expl Neurol 1991; 28:139–45
62. June CH, Contreras CE, Perrin LH, et al. Circulating and tissue-bound immune complex formation in murine malaria. J Immunol 1979;122: 2154–61
63. Wolburg H, Paulus W. Choroid plexus: Biology and pathology. Acta Neuropathol 2010;119:75–88
64. Moore GR, Stadelmann-Nessler C. Demyelinating diseases. In: Love S, Perry A, Ironside J, Budka H, eds. Greenfield's Neuropathology. 9th Edition. Boca Raton, FL: CRC Press 2015:1297–412.
65. Miklossy J, Kraftsik R, Pillevuit O, et al. Curly fiber and tangle-like inclusions in the ependyma and choroid plexus–A pathogenetic relationship with the cortical Alzheimer-type changes? J Neuropathol Exp Neurol 1998;57:1202–12
66. Glassock RJ. Diagnosis and natural course of membranous nephropathy. Semin Nephrol 2003;23:324–32
67. Mullins RF, Schoo DP, Sohn EH, et al. The membrane attack complex in aging human choriocapillaris: Relationship to macular degeneration and choroidal thinning. Am J Pathol 2014;184:3142–53
68. Johnson LV, Ozaki S, Staples MK, et al. A potential role for immune complex pathogenesis in drusen formation. Exp Eye Res 2000;70:441–9
69. McHarg S, Clark SJ, Day AJ, et al. Age-related macular degeneration and the role of the complement system. Mol Immunol 2015;67:43–50
70. Zhang Y, Pardridge WM. Mediated efflux of IgG molecules from brain to blood across the blood-brain barrier. J Neuroimmunol 2001;114: 168–72
71. Brightman MW, Klatzo I, Olsson Y, et al. The blood-brain barrier to proteins under normal and pathological conditions. J Neurol Sci 1970;10: 215–39
72. Jacobsen M, Jacobsen GK, Clausen PP, et al. Intracellular plasma proteins in human fetal choroid plexus during development. II. The distribution of prealbumin, albumin, alpha-fetoprotein, transferrin, IgG, IgA, IgM, and alpha 1-antitrypsin. Brain Res 1982;255:251–62
73. Møllgård K, Jacobsen M, Jacobsen GK, et al. Immunohistochemical evidence for an intracellular localization of plasma proteins in human foetal choroid plexus and brain. Neurosci Lett 1979;14:85–90
74. Shrestha B, Paul D, Pachter JS. Alterations in tight junction protein and IgG permeability accompany leukocyte extravasation across the choroid plexus during neuroinflammation. J Neuropathol Exp Neurol 2014;73: 1047–61
75. Henderson AL, Lindorfer MA, Kennedy AD, et al. Concerted clearance of immune complexes bound to the human erythrocyte complement receptor: Development of a heterologous mouse model. J Immunol Methods 2002;270:183–97
76. Rojko JL, Evans MG, Price SA, et al. Formation, clearance, deposition, pathogenicity, and identification of biopharmaceutical-related immune complexes: Review and case studies. Toxicol Pathol 2014;42:725–64
77. Selmaj K, Pawlowska Z, Walczak A, et al. Corpora amylacea from multiple sclerosis brain tissue consists of aggregated neuronal cells. Acta Biochim Pol 2008;55:43–9